

CosPGD: a unified white-box adversarial attack for pixel-wise prediction tasks

Shashank Agnihotri¹ Margret Keuper^{1,2}, ¹University of Siegen, ²Max Planck Institute for Informatics

Abstract

While neural networks allow highly accurate predictions in many tasks, their lack in robustness towards even slight input perturbations hampers their deployment in many real-world applications. Recent research towards evaluating the robustness of neural networks such as the seminal *projected gradient descent* (PGD) attack and subsequent works and benchmarks have therefore drawn significant attention. Yet, such methods focus predominantly on classification tasks, while only a few approaches specifically address the analysis of pixel-wise prediction tasks such as semantic segmentation, optical flow, or disparity estimation. One notable exception is the recently proposed SegPGD attack, which could showcase the importance of pixel-wise attacks for evaluating semantic segmentation. While SegPGD is limited to pixel-wise classification (i.e. segmentation), in this work, we propose CosPGD, a novel white-box adversarial attack that allows to optimize dedicated attacks for any pixel-wise prediction task in a unified setting. It leverages the cosine similarity between the predictions and ground truth to extend directly from classification tasks to regression settings. Further, we empirically show the superior performance of CosPGD for semantic segmentation as well as for optical flow and disparity estimation.

1. Introduction

Neural networks (NNs) have been gaining popularity for estimating solutions to various complex tasks including numerous vision tasks like classification (Krizhevsky et al., 2012; He et al., 2015; Xie et al., 2016; Liu et al., 2022), semantic segmentation (Ronneberger et al., 2015; Zhao et al., 2016), or disparity (Li et al., 2020a) and optical flow (Fischer et al., 2015; Ilg et al., 2016; Teed & Deng, 2020) estimation. However, NNs are inherently black-box function approximators (Buhrmester et al., 2019), known to find shortcuts to map the input to a target distribution (Geirhos et al., 2020) or to learn biases (Geirhos et al., 2018). Thus we have limited information on the quality of representations learned

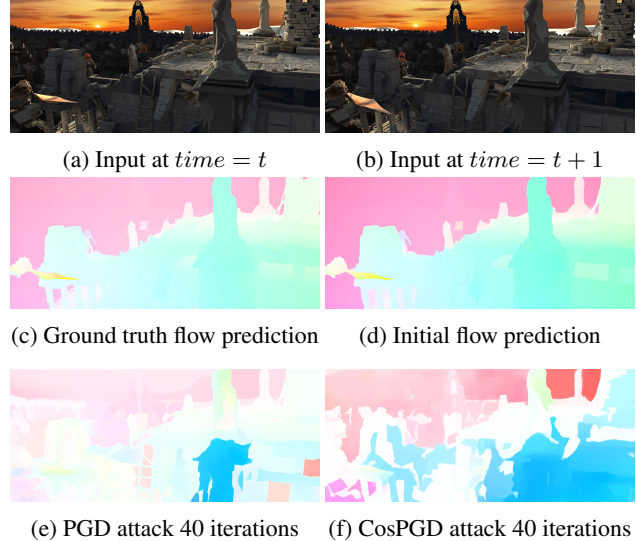


Figure 1: A comparison of optical flow predictions using RAFT (Teed & Deng, 2020) on Sintel (Butler et al., 2012; Wulff et al., 2012) validation images changed due to PGD attack in Fig. 1e to CosPGD attack in Fig. 1f w.r.t. the initial flow prediction shown in Fig. 1d. Fig. 1c shows the optical flow ground truth. Figs. 1a and 1b show 2 consecutive frames for which the optical flow was predicted. For the same perturbation size and amount of iterations, the proposed CosPGD alters the estimated optical flow more strongly and even changes the background motion direction.

by the network and despite their highly accurate predictions in many tasks, neural network based models tend to lack robustness towards even slight input perturbations. This draws skepticism on the real-world applicability of neural networks. Recent research towards evaluating the robustness of neural networks such as FGSM (Goodfellow et al., 2014), the *projected gradient descent* (PGD) attack (Kurakin et al., 2017) and subsequent works such as (Schrodi et al., 2022; Croce & Hein, 2020; 2021) and benchmarks (Croce et al., 2021) have therefore attracted significant attention. An adversarial attack adds a crafted, small (epsilon-sized) perturbation to the input of a neural network that aims to alter the prediction. Due to the practical relevance to evaluate and analyze neural network models, such attacks have been extensively developed and studied (Goodfellow et al., 2014;

Kurakin et al., 2017; Wong et al., 2020b; Madry et al., 2017; Moosavi-Dezfooli et al., 2015; Kurakin et al., 2016). Yet, existing approaches predominantly focus on attacking image classification models. However, arguably, the robustness of models for pixel-wise prediction tasks is highly relevant for many safety-critical applications such as motion estimation in autonomous driving or medical image segmentation. Li et al. (2020b) in their work, show that perturbations from an adversarial attack, like PGD can be utilized in training better segmentation models for medical applications. The application of existing attacks to pixel-wise prediction tasks such as semantic segmentation or optical flow estimation is possible in principle (e.g. as in (Arnab et al., 2017)), albeit carrying only limited information since the pixel-specific loss information is not leveraged. In Fig. 1, we illustrate this effect on the task of optical flow estimation and show that global attacks such as PGD (Fig. 1(e)) can fool the network predictions to some extent. However, motion boundaries and coarse motion directions are mostly preserved. Recently, Gu et al. showed that harnessing pixel-wise information for adversarial attacks leads to much stronger attacks for semantic segmentation tasks.

In this work, we propose CosPGD, a novel white-box adversarial attack. CosPGD uses the cosine-similarity between the prediction and target for each pixel, to generate an adversarial attack. Due to its principled formulation, CosPGD can be used for a wide range of pixel-wise prediction tasks, beyond semantic segmentation. Fig. 1(f) shows its effect on optical flow estimation. CosPGD uses the pixel-precise loss information is therefore significantly stronger than global attacks like PGD. Since it can leverage the posterior distribution of the prediction for the loss computation, it can also outperform SegPGD on semantic segmentation. The main contributions of this work are as follows:

- We propose a novel white-box adversarial attack, CosPGD which can be used to attack all pixel-wise prediction tasks.
- We show that CosPGD is stronger than other attacks on three different downstream tasks: semantic segmentation, optical flow estimation, and disparity estimation.
- For semantic segmentation, we compare our method to another recently proposed adversarial attack, SegPGD that also uses pixel-wise information for generating attacks. CosPGD can outperform SegPGD by a significant margin.

2. Related work

The vulnerability of NNs to adversarial attacks was first explored in Goodfellow et al. (2014) for image classification, proposing the Fast Gradient Sign Method (FGSM).

FGSM is a single-step (one-iteration) white-box adversarial attack that perturbs the input in the direction of its gradient, generated from backpropagating the loss, with a small step size, such that the model prediction becomes incorrect. Due to its fast computation, it is still a widely used approach. Numerous subsequent works have been directed towards generating effective adversarial attacks for diverse tasks including NLP (Morris et al., 2020; Ribeiro et al., 2018; Iyyer et al., 2018), or 3D tasks (Zhang et al., 2021; Sun et al., 2021). Yet, the high input dimensionality of image classification models results in the striking effectiveness of adversarial attacks in this field (Goodfellow et al., 2014). A vast line of work has been dedicated to assessing the quality and robustness of representations learned by the network, including the curation of dedicated evaluation data for particular tasks (Kang et al., 2019; Hendrycks & Dietterich, 2019; Hendrycks et al., 2019) or the crafting of effective adversarial attacks. Patch attacks perturb a localized region in the image (e.g. (Brown et al., 2017)), while methods such as proposed in (Goodfellow et al., 2014; Kurakin et al., 2017; Madry et al., 2017; Wong et al., 2020b; Moosavi-Dezfooli et al., 2015; Croce & Hein, 2020; Andriushchenko et al., 2020; Carlini & Wagner, 2017; Rony et al., 2019) argue in a Lipschitz continuity motivated way that a robust network’s prediction should not change drastically if the perturbed image is within the epsilon-ball of the original image and thus optimize attacks globally within the epsilon neighborhood of the original input. Our proposed CosPGD approach follows this line of work.

White-box attacks assume full access to the model and its gradients (Goodfellow et al., 2014; Kurakin et al., 2017; Madry et al., 2017; Wong et al., 2020b; Gu et al., 2022a; Moosavi-Dezfooli et al., 2015) while black-box attacks optimize the perturbation in a randomized way (Andriushchenko et al., 2020; Ilyas et al., 2018). The proposed CosPGD derives its optimization objective from PGD (Kurakin et al., 2017) and is a white-box attack.

Further, one can distinguish between *targeted attacks* (e.g. (Wong et al., 2020a; Gajjar et al., 2022; Schmalfuss et al., 2022)) that turn the network predictions towards a specific target and *untargeted attacks* that optimize the attack to cause any incorrect prediction. Projected Gradient Descent (PGD) (Kurakin et al., 2017) for example can be used in both settings (Vo et al., 2022). While the proposed CosPGD is related to PGD, we focus in this work on untargeted attacks.

While previous attacks predominantly focus on classification tasks, only a few approaches specifically address the analysis of pixel-wise prediction tasks such as semantic segmentation, optical flow, or disparity estimation. Notable exceptions of pixel-wise white-box adversarial attacks are proposed in (Gu et al., 2022a; Schmalfuss et al., 2022). For

example, the recent SegPGD (Gu et al., 2022a) attack could showcase the importance of pixel-wise attacks for semantic segmentation. PCFA (Schmalfuss et al., 2022) was applied to the estimation of optical flow and specifically minimizes the end-point error (*ep*) to a target flow field. In this work, we propose CosPGD to provide a principled approach for untargeted adversarial attacks that can be applied to a wide range of pixel-wise prediction tasks in a unified setting.

Our work is inspired by the SegPGD method and based on the untargeted optimization formulated in Projected Gradient Descent(PGD) (Kurakin et al., 2017). PGD in its formulation is very similar to FGSM, i.e. it aims to increase the network’s loss for an image by adding epsilon-bounded noise. Yet, it is significantly more expensive to optimize than FGSM since it is allowed not one but multiple optimization steps. We explain PGD in more detail in section 3. SegPGD (Gu et al., 2022a) extends upon PGD for semantic segmentation by considering the loss per pixel. For effective optimization, it splits the model’s predicted segmentation mask into correctly classified and incorrectly classified pixels, by comparing it to the ground truth segmentation mask. Thus, the loss is scaled over the iterations and the attack does not continue to increase the loss on already flipped pixel labels. While SegPGD improves upon previous adversarial attacks, it is limited to pixel-wise *classification* tasks (i.e. semantic segmentation) and cannot directly be extended to regression-based tasks like disparity estimation or optical flow estimation. Thus, we propose CosPGD. CosPGD uses the pixel-wise cosine similarity between the predictions and the targets to scale the loss for each pixel so that it can be applied to classification and regression tasks in a principled way. Further, the cosine similarity can be evaluated on the prediction scores for pixel-wise classification tasks and thereby leverage even more information from the network. Thus CosPGD outperforms SegPGD when attacking semantic segmentation models.

3. Method

CosPGD is an iterative white-box untargeted attack that utilizes pixel-wise cosine similarity to generate strong adversarial examples. The method is inspired by SegPGD(Gu et al., 2022a) and is an effective extension of PGD for all pixel-wise predictions tasks with the same attack step as PGD, given in equation (1) and in Kurakin et al. (2017); Gu et al. (2022a).

$$\begin{aligned} \mathbf{X}^{\text{adv}_{t+1}} &= \phi^\epsilon(\mathbf{X}^{\text{adv}_t} + \\ &\quad \alpha * \text{sign}(\nabla_{\mathbf{X}^{\text{adv}_t}} L(f_{\text{net}}(\mathbf{X}^{\text{adv}_t}), \mathbf{Y}))) \end{aligned} \quad (1)$$

where $\mathbf{X}^{\text{adv}_{t+1}}$ is a new adversarial example for time step $t + 1$, generated using $\mathbf{X}^{\text{adv}_t}$, the adversarial example at time step t , \mathbf{Y} is the ground truth label, α is the step size for the perturbation, and the function ϕ^ϵ is clipping the gen-

erated example in ϵ -ball. Its purpose is to restrict the attack according to the l_∞ -norm constraint. $\nabla_{\mathbf{X}^{\text{adv}_t}} L(\cdot)$ denotes the gradient of $\mathbf{X}^{\text{adv}_t}$ generated by backpropagating the loss and is used to determine the direction of the perturbation step. SegPGD (Gu et al., 2022a) extends this formulation to tensor-valued predictions and labels $\mathbf{Y} \in \mathbb{R}^{H \times W \times M}$ for images of size $H \times W$ and categorical M output classes. This allows specifically optimizing perturbations on pixels on which the loss is low instead of only having access to the total loss per image.

Loss scaling in SegPGD When optimizing an adversarial attack, the pixels which are already misclassified by the model are less relevant than pixels correctly classified by the model because the intention of the attack is to make the model misclassify as many pixels as possible while perturbing the input inside the ϵ -ball. However, Gu et al. (2022a) argues that over iterations, as the number of misclassified pixels increases, the attack starts losing effectiveness if it only focuses on correctly classified pixels. Thus, the authors propose scaling the loss over iterations such that the scaling of the loss for correctly classified pixels is inversely proportional to the scaling of the loss for the incorrectly classified pixels. Initially, the loss for the correctly classified pixels is scaled higher, compared to the loss for the incorrectly classified pixels. Then, over iterations, the scaling of the loss for the correctly classified pixels is reduced (compare equation (4) in SegPGD (Gu et al., 2022b)). This avoids the concern of the attack becoming benign after a few iterations. However, splitting the pixels into two categories of correct and incorrectly classified ones limits the application to pixel-wise classification tasks like semantic segmentation. For pixel-wise regression tasks like optical flow, and surface normal prediction such an absolute measure of correctness would fail. Further, comparing the pixel-wise labels after taking the argmax only provides limited information from the network prediction. Thus, we argue that the scope of the categories needs to be expanded such that it can encompass the similarity between the predictions and the label.

CosPGD The aim of the proposed CosPGD approach is to facilitate the effective application of PGD-like adversarial attacks to pixel-wise prediction tasks in a principled way. To cope with the above-sketched problem addressed in SegPGD, we propose a unified way to scale the loss in classification and regression settings. Specifically, we aim to penalize pixel-wise in proportion to the pixel-wise predictions’ similarity to the ground truth, while also accounting for the decrease in similarity over iterations. We propose to use the cosine similarity as this measure, as it satisfies the desired properties.

The cosine similarity between the model predictions and target (ground truth) is calculated as shown in equation (2)

Algorithm 1 Algorithm for generating adversarial examples using CosPGD.

Require: model $f_{\text{net}}(\cdot)$, clean samples $\mathbf{X}^{\text{clean}}$, perturbation range ϵ , step size α , attack iterations T , ground truth \mathbf{Y}

```

 $\mathbf{X}^{\text{adv}_0} = \mathbf{X}^{\text{clean}} + \mathcal{U}(-\epsilon, +\epsilon)$                                  $\triangleright$  initialize adversarial example
for  $t \leftarrow 1$  to  $T$  do                                                  $\triangleright$  loop over attack iterations
     $P = f_{\text{net}}(\mathbf{X}^{\text{adv}_{t-1}})$                                           $\triangleright$  make predictions
     $\text{cossim} \leftarrow \text{CosineSimilarity}(P, \mathbf{Y})$                           $\triangleright$  compute cosine similarity
     $L_{\text{cos}} \leftarrow \text{cossim} * L(P, \mathbf{Y})$                                  $\triangleright$  loss for example updates
     $\mathbf{X}^{\text{adv}_t} \leftarrow \mathbf{X}^{\text{adv}_{t-1}} + \alpha * \text{sign}(\nabla_{\mathbf{X}^{\text{adv}_{t-1}}} L_{\text{cos}})$   $\triangleright$  update adversarial examples
     $\mathbf{X}^{\text{adv}_t} \leftarrow \phi^{\epsilon}(\mathbf{X}^{\text{adv}_t})$                                           $\triangleright$  clip into  $\epsilon$ -ball of clean image
end for

```

for each output pixel location:

$$\cos(\overrightarrow{\text{pred}}, \overrightarrow{\text{target}}) = \frac{\overrightarrow{\text{pred}} \cdot \overrightarrow{\text{target}}}{\|\overrightarrow{\text{pred}}\| \cdot \|\overrightarrow{\text{target}}\|} \quad (2)$$

Where, $\overrightarrow{\text{pred}}$ are the predictions of a network $f_{\text{net}}(\cdot)$ for a position, and $\overrightarrow{\text{target}}$ are the target predictions or ground truth at the same position. CosPGD being an untargeted attack, intends to drive the model's predictions away from the model's intended target(ground truth). For pixel-wise prediction tasks like disparity estimation, optical flow, etc. the predictions, and targets are vectors containing information for each pixel.

In the case of semantic segmentation, we vectorize the target by generating a *one-hot encoded vector* of the target and we vectorize the predictions, by calculating the sigmoid of the predictions before taking the argmax as shown in equation (3).

$$\overrightarrow{\text{pred}} = \text{sigmoid}^1(f_{\text{net}}(\mathbf{X})) \quad (3)$$

Similar to (Gu et al., 2022a), \mathbf{X}^{adv} is initialized to the clean input sample $\mathbf{X}^{\text{clean}}$ with added randomized noise in the range $[-\epsilon, +\epsilon]$, ϵ being the maximum allowed perturbation. Over attack iterations $\mathbf{X} = \mathbf{X}^{\text{adv}_t}$, the adversarial example generated at iteration t , such that $t \in [1, T]$, where T is the total number of attack iterations.

As discussed, we finally propose to scale the loss using this cosine similarity (cossim) $\cos(\overrightarrow{\text{pred}}, \overrightarrow{\text{target}})$. Such that, pixels, where the network predictions are closer to the target, have a higher similarity(approaching 1) and thus higher loss. While pixels with lower similarity, have a lower loss but are not rendered benign. Thus, the final loss over all pixels is calculated as shown in equation 4, then this loss is back propagated to obtain gradients over the sample to perform the adversarial attack as shown in equation (1) using L_{cos}

¹ $\text{sigmoid}(x) = \frac{1}{1 + e^{-x}}$

instead of L .

$$L_{\text{cos}} = \frac{1}{H \times W} \sum_{H \times W} \cos(\overrightarrow{\text{pred}}, \overrightarrow{\text{target}}) \cdot L(f_{\text{net}}(\mathbf{X}^{\text{adv}_t}), \mathbf{Y}) \quad (4)$$

Where, H and W are the height and width of a sample \mathbf{X} . The flow of CosPGD is summarized in algorithm 1.

4. Experiments

For demonstrating the wide applicability of CosPGD, we conduct our experiments on three distinct downstream tasks: semantic segmentation, optical flow estimation, and disparity estimation. For semantic segmentation, we compare CosPGD to SegPGD, while for optical flow estimation and disparity estimation, we compare CosPGD to PGD. We can observe that CosPGD outperforms SegPGD and PGD, respectively. We also evaluate one-step CosPGD, where CosPGD is only optimized with a single update step similar to FGSM, to the original FGSM attack (Goodfellow et al., 2014) for all considered downstream tasks. We show that one-step CosPGD is as strong as or stronger than FGSM.

4.1. Experimental setup

When comparing CosPGD we use the same ϵ for CosPGD as FGSM, SegPGD ($\epsilon = 0.03$), or PGD ($\epsilon = 0.03$). For SegPGD, we follow the work by Gu et al. (2022a) and set the step size $\alpha = 0.01$. Since CosPGD directly compares the prediction vectors to target vectors, as opposed to SegPGD which compares final masks, the magnitudes of the similarities are much slower. Thus, this is compensated with a higher step size $\alpha = 0.15$. We ablate over this design choice in Sec.B.

Semantic Segmentation. We use the PASCAL VOC 2012 (Everingham et al.) dataset which contains 20 classes object classes and one background class, with 1464 training images, and 1449 validation images. We follow common practice(Hariharan et al., 2015; Gu et al., 2022a; Zhao, 2019;

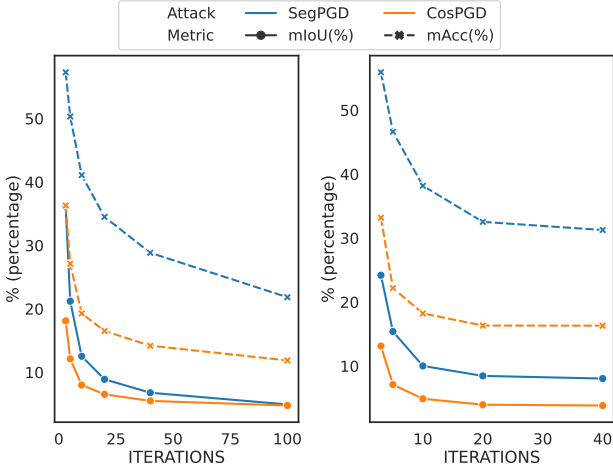


Figure 2: Comparison of performance of CosPGD to SegPGD for semantic segmentation over PASCAL VOC2012 validation dataset using UNet (left) and PSP-Net (right). We also report these results in Tab. 3

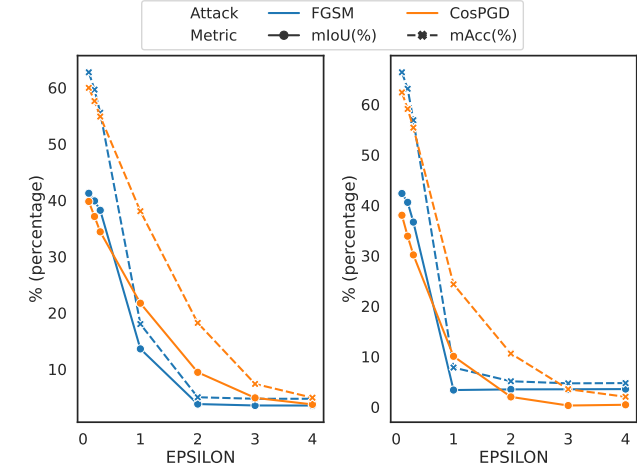


Figure 3: Comparison of performance of one-step CosPGD to FGSM for semantic segmentation over PASCAL VOC2012 validation dataset using UNet(left) and PSP-Net(right). We also reported the results in Tab. 4.

Zhao et al., 2017), and use work by Hariharan et al. (2011), augmenting the training set to 10,582 images. We test on the validation dataset. Architectures used for our evaluations are UNet (Ronneberger et al., 2015), and PSPNet (Zhao et al., 2016; 2017). We report the mean Intersection over Union (mIoU) and mean pixel accuracy (mAcc) as metrics for comparison.

Optical flow estimation. We use RAFT(Teed & Deng, 2020) for our evaluations and follow the evaluation procedure used by Teed & Deng (2020). Evaluations are performed on KITTI2015 (Menze & Geiger, 2015) and MPI Sintel (Butler et al., 2012; Wulff et al., 2012) validation datasets. We use the networks pre-trained on FlyingChairs (Dosovitskiy et al., 2015), and FlyingThings (Mayer et al., 2016) and fine-tuned on training datasets of the specific evaluation, as provided by Teed & Deng (2020). For Sintel, we report the end-point error (*epe*) on both clean and final subsets, while for KITTI15 we report the *epe* and *f1 – all*.

Disparity and occlusion estimation. We consider the STTR-light (Li et al., 2020a) (STereoTRansformer) architecture for disparity estimation on the FlyingThings3D (Mayer et al., 2016) dataset. We follow the training and evaluation process, as done by Li et al. (2020a). We report the absolute error (*epe*), and 3px error (*px error*) and for occlusion estimation, we report the mean *IoU*.

4.2. Semantic segmentation

We report the comparison of CosPGD to the recently proposed SegPGD in Fig 2. We observe that using the cosine similarity between the vectorized predictions and targets

yields a much stronger attack compared to naive equality between the predicted and target segmentation masks.

This is consistent across the number of attack iterations, as CosPGD fools the networks into making wrong predictions much better than SegPGD. This claim is supported by both metrics mIoU and mAcc being much lower for CosPGD when compared to SegPGD.

In Fig 3 we compare the one-step version of CosPGD (executing a single gradient step) to FGSM. We observe that at low epsilon values, CosPGD is better than FGSM, while FGSM is stronger for mid-level-sized perturbations. However, at these epsilon values, FGSM is not an effective attack, as the examples generated by FGSM are very noisy. This can be qualitatively seen in Fig 5. Moreover, this can also be observed by quantitative results in Fig 3, where the mIoU and mAcc improve marginally as perturbation size (ϵ) increases.

In contrast, we observe for CosPGD, the drop is much smoother and as shown in Fig 5 the samples generated are comparatively less noisy. At a comparatively low value of ϵ (=0.2), examples generated by FGSM and one-step CosPGD have similar quality (denoted by their PSNR values) and visually look similar. Nevertheless, CosPGD is succeeding in fooling the model to a greater extent, when compared to FGSM, leading to significantly lower mIoU of the predictions. Fig 5 shows, at high ϵ (=2.0), adversarial examples generated by FGSM have a very low PSNR, especially when compared to examples generated by CosPGD at the same epsilon value. Thus, in the case of an FGSM attack, the model is unable to find the object and is simply predicting the entire image as background. In comparison,

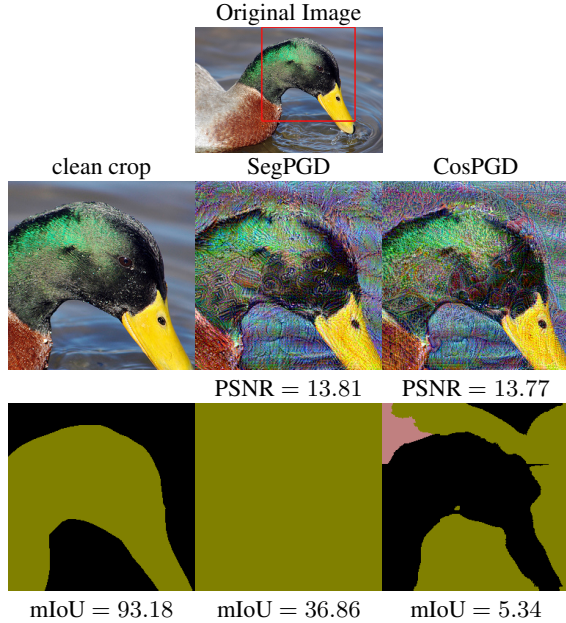


Figure 4: Zoomed in comparison of adversarial examples generated by SegPGD (middle) and CosPGD (right) after 20 attack iterations and the resulting segmentation masks. The left column shows the clean crop used to generate the adversary and its resulting segmentation mask predicted by UNet. The quality of the generated samples can be judged by the PSNR values (in db) of the respective samples w.r.t. the clean input sample. While SegPGD mostly attacks the background, CosPGD can alter both foreground and background labels and further decrease the segmentation mIoU while the PSNR of both attacked images is comparable.

when the model is attacked with one-step CosPGD, due to better image quality, the model is still able to find an object. Furthermore, due to the effectiveness of the attack, it is mislabelling the classes and incorrectly predicting the segmentation mask. Thus, one-step CosPGD is significantly more effective as an adversarial attack, even with one-step when compared to its counterpart FGSM, across all ϵ s.

Moreover, we note in Fig 4, that after 20 attack iterations, the adversarial examples generated by both SegPGD and CosPGD look similar to a human eye, even having very similar PSNR values denoting the quality of the images. The merits of CosPGD and the demerits of SegPGD are qualitatively highlighted by Fig 4. The model, when predicting on the clean image, is able to correctly predict the segmentation mask and object class, with a high $mIoU = 93.18$. When the model is attacked with SegPGD, it simply predicts the entire image as a duck (the object class label in the example), without altering the object class label prediction. However, when attacked with CosPGD, with the same perturbation size ($\epsilon = 0.03$) and the same iterations as SegPGD, and the image quality being very similar to that generated by

SegPGD attack, the predictions are very different. CosPGD is able to fool the model into predicting the reverse predictions for almost all pixels. We see in Fig 4, that after the CosPGD attack, the model is predicting the duck pixels are background class, while most of the background is being predicted as the object class, while in a small region, the object class label being predicted is not even present in the image. Quantitatively, by the performance comparison of $mIoU$ and $mAcc$, as shown in Fig 2, we conclude that CosPGD is a stronger and more effective attack than SegPGD for semantic segmentation.

4.3. Optical Flow

We observe in Fig 6, the initial optical flow estimation by the model is very close to the ground truth. When attacking the model with a strong adversarial attack like PGD, designed originally for classification tasks, the model is fooled marginally even as the intensity of the attack is increased to 40 iterations. In table 1, we report the quantitative results and observe that as the attack intensity (iterations) is increased, the performance of the model worsens. However, figures 6b, 6c show qualitatively that the model predictions are not significantly different from the initial predictions. As in the example in Fig. 6, when attacked by PGD for 5 iterations, the model is able to predict the motion of the car and the background with significant correctness, thus worsening the epe from 0.64 (initial flow prediction) to only 1.35 (PGD attack with 5 iterations).

The limited effectiveness of the PGD attack is further highlighted in Fig. 6c, where even after 40 attack iterations, the epe is only worsened to 12.93, this is also visible in the flow predictions of the model, as it is still able to predict the motion of the car and the background with some correctness. This is in contrast to when the model is attacked using CosPGD, a method that utilizes pixel-wise information. In Fig. 6e, we observe that even at a low intensity of the attack (5 iterations), the model predictions are significantly different from the initial predictions. The model is incorrectly predicting the motion of the pixels around the moving car. And at high attack intensity, as shown in Fig. 6f with 40 iterations, the model's optical flow predictions are significantly inaccurate and exceedingly different from both, the initial predictions and the ground truth. The model fails to differentiate the moving car from its background and the road. In a real-world scenario, this vulnerability of the model to a small perturbation ($\epsilon = 0.03$) could be hazardous.

A similar observation is made for the Sintel dataset, in Fig 1, as explained earlier in section 1. The dominance of CosPGD over PGD, as an adversarial attack, can be quantitatively observed in table 1.

We also compare one-step CosPGD (i.e. CosPGD with only

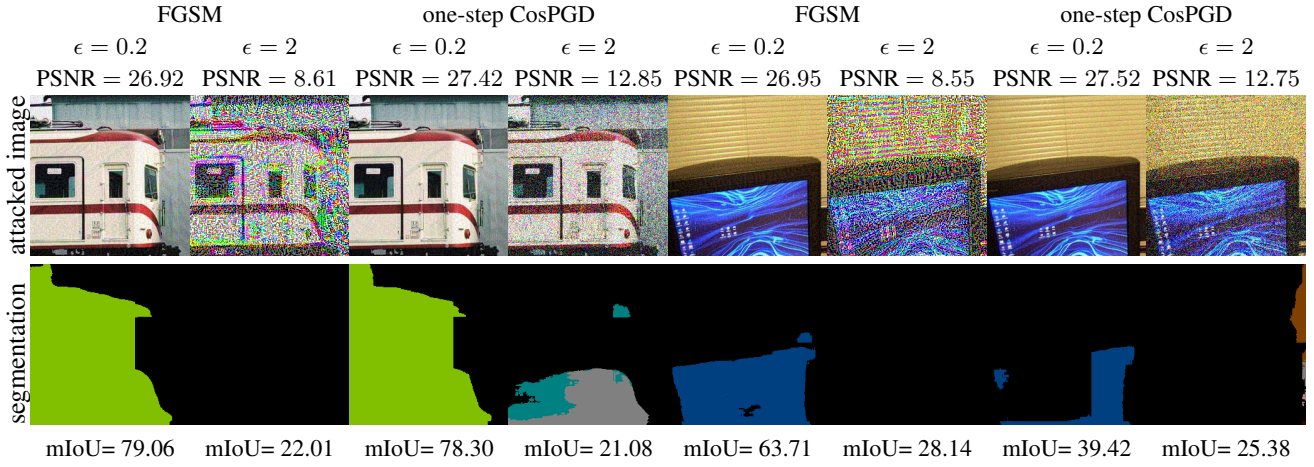


Figure 5: Comparing adversarial samples generated using crops from input by FGSM and one-step CosPGD at low and high values of epsilons ($\epsilon=0.2$ and 2). We observe that for $\epsilon = 0.2$, FGSM and CosPGD both produce samples that do not look perturbed to the human eye. However, at $\epsilon = 2$, there is a significant difference in the quality of samples produced by both methods. While, samples generated by CosPGD appear noisy to an expected level for high attack intensities, the samples generated by FGSM are much more perturbed. This can be quantitatively shown using Peak Signal-to-Noise Ratio (PSNR, in db) values↑ for the generated samples w.r.t. the clean(unperturbed) crops. At the same time, CosPGD causes lower mIoU.

Table 1: Comparison of performance of CosPGD to PGD for optical flow estimation over KITTI15 and Sintel validation datasets using RAFT for different numbers of attack iterations. CosPGD systematically outperforms PGD for both datasets, in terms of *epe* and *f1 – all* (for KITTI15) across all tested numbers of iterations.

Attack	KITTI15				Sintel			
Iterations	PGD		CosPGD		PGD		CosPGD	
	epe↑	f1-all↓	epe↑	f1-all↓	clean epe↑	final epe↑	clean epe↑	final epe↑
3	2.03	7.86	4.00	22.01	1.06	1.89	2.85	5.01
5	2.35	9.85	5.93	35.66	1.29	2.37	4.55	8.51
10	3.25	14.89	12.28	60.91	1.89	3.87	10.01	18.34
20	5.51	23.12	32.85	79.33	3.40	8.19	25.52	49.25
40	12.93	33.36	116.28	87.40	7.74	21.89	87.22	140.97

a single attack iteration as in FGSM) to FGSM in table 5 on the RAFT model in Sec. A.2. We observe that with the same ϵ and step size as FGSM, CosPGD is at par or marginally stronger than FGSM across all epsilons and datasets, for example increasing the final end-point-error to 12.045 for epsilon = 8.0 on Sintel. Thus, we demonstrate the effectiveness of the CosPGD attack for the downstream task of optical flow.

4.4. Disparity Estimation

We compare CosPGD to PGD for the task of disparity estimation and occlusion detection and report the results in Table 2. Here we observe the *epe* and pixel error (*px error*) values for disparity estimation are significantly higher when the model is attacked with CosPGD compared to an attack by PGD, across attack iterations. For the PGD attack, as

the attack intensity is increased by increasing the number of attack iterations, we observe the model predictions for disparity estimation worsening as the *epe* and *px error* values increase proportionally while the IoU of occlusion detection drops as well. In the case of the CosPGD attack, when compared to PGD with the same attack iterations as PGD (with the same perturbation size, $\epsilon = 0.03$), the attack is significantly stronger as the *epe* and *px error* values are comparatively much higher. Notably, even the *IoU* of occlusion detection by the model is marginally lower when it is attacked with CosPGD, as opposed to PGD. This is despite the fact that the task of occlusion detection on FlyingThings3D is rather easy, with the model initially predicting it with an accuracy of 98.08%. Thus, this experiment demonstrates the strength of CosPGD as an adversarial attack even for this pixel-wise prediction task.

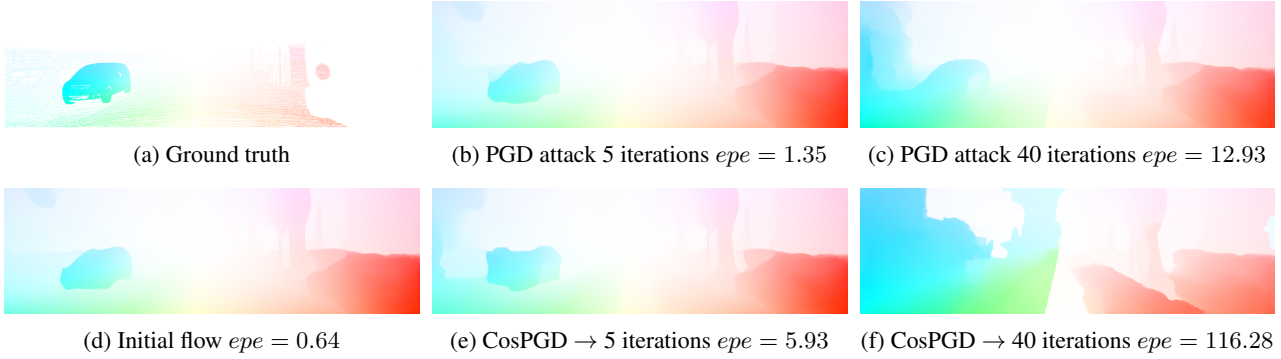


Figure 6: Comparing PGD and CosPGD attack on RAFT using KITTI15 validation set over various iterations. Fig.6a shows the ground truth prediction and fig.6d shows the initial optical flow estimation by the network before adversarial attacks. Figures 6b and 6c show flow predictions after PGD attack over 5 and 40 iterations respectively, while figures 6e and 6f show flow predictions after CosPGD attack over 5 and 40 iterations respectively. CosPGD significantly changes the overall structure of the optical flow field. For example, the shape of the car remains visible in the flow estimations after the PGD attack, while CosPGD alters the perceivable shapes in the estimated flow resulting in a significantly higher epe for CosPGD.

Table 2: Comparing performance of CosPGD to PGD for Disparity Estimation over FlyingThings3D test dataset using STTR-light. The proposed CosPGD is stronger than PGD in all three metrics and across tested numbers of attack iterations.

# Attack iterations	PGD			CosPGD		
	$epe \uparrow$	$\text{IoU}(\%) \downarrow$	$\text{px error} \uparrow$	$epe \uparrow$	$\text{IoU}(\%) \downarrow$	$\text{px error} \uparrow$
3	5.7675	97.61	0.4802	38.7281	97.40	0.8073
5	9.5692	97.52	0.6813	73.8921	97.37	0.9240
10	19.1480	97.41	0.8636	136.2433	97.37	0.9842
20	45.2787	97.32	0.9540	212.3926	97.31	0.9967
40	104.4950	97.24	0.9881	343.0897	97.05	0.9989

5. Conclusion

In this work, we demonstrated across different downstream tasks and architectures that our proposed adversarial attack, CosPGD, is significantly more effective than other existing and commonly used adversarial attacks on several pixel-wise prediction tasks. By comparing CosPGD to attacks like FGSM and PGD that were originally proposed for image classification tasks, we expanded on the work by Gu et al. (2022a) and highlighted the need and effectiveness of attacks specifically designed for pixel-wise prediction tasks beyond segmentation. We illustrated the intuition behind using cosine similarity as a measure for generating stronger adversaries and leveraging more information from the model and backed it with experimental results from three different downstream tasks. This further highlights the simplicity of and principled formulation of CosPGD, thus making it applicable to a wide range of pixel-wise prediction tasks.

Limitations. Similar to most white-box adversarial attacks(Goodfellow et al., 2014; Kurakin et al., 2017; Madry et al., 2017; Wong et al., 2020b; Gu et al., 2022a), CosPGD currently requires ground truth predictions for generating

adversarial examples. While this is beneficial for generating adversaries, it limits the applications as many benchmark datasets (Menze & Geiger, 2015; Butler et al., 2012; Wulff et al., 2012; Everingham et al.) do not provide the ground truth for test data. Evaluations on the validation datasets certainly show the merit of the attack method. Yet, it would be interesting to study the attack on test images as well, due to the potential slight distribution shifts pre-existing in the test data.

Future Work. In current evaluations, CosPGD is an untargeted attack, using information from the model it is intending to attack without targeting a particular desired prediction. It would be interesting to study the effectiveness of CosPGD as a targeted attack. Further, an analysis of the performance of CosPGD compared to other l_∞ and l_p norm-constrained attacks against adversarial defense mechanisms, such as those discussed by Grabinski et al. (2022); Xu et al. (2019) would be an interesting case study. Many strong adversarial attacks are also good methods for adversarial training (Kurakin et al., 2017; 2016; Gu et al., 2022a). Thus a future direction will be to study the adversarial robustness of models trained with CosPGD.

References

Andriushchenko, M., Croce, F., Flammarion, N., and Hein, M. Square attack: a query-efficient black-box adversarial attack via random search. 2020.

Arnab, A., Miksik, O., and Torr, P. H. S. On the robustness of semantic segmentation models to adversarial attacks, 2017. URL <https://arxiv.org/abs/1711.09856>.

Brown, T. B., Mané, D., Roy, A., Abadi, M., and Gilmer, J. Adversarial patch, 2017. URL <https://arxiv.org/abs/1712.09665>.

Buhrmester, V., Münch, D., and Arens, M. Analysis of explainers of black box deep neural networks for computer vision: A survey, 2019. URL <https://arxiv.org/abs/1911.12116>.

Butler, D. J., Wulff, J., Stanley, G. B., and Black, M. J. A naturalistic open source movie for optical flow evaluation. In A. Fitzgibbon et al. (Eds.) (ed.), *European Conf. on Computer Vision (ECCV)*, Part IV, LNCS 7577, pp. 611–625. Springer-Verlag, October 2012.

Carlini, N. and Wagner, D. Towards evaluating the robustness of neural networks. In *2017 ieee symposium on security and privacy (sp)*, pp. 39–57. IEEE, 2017.

Croce, F. and Hein, M. Reliable evaluation of adversarial robustness with an ensemble of diverse parameter-free attacks. In *ICML*, 2020.

Croce, F. and Hein, M. Mind the box: l_1 -apgdr for sparse adversarial attacks on image classifiers. In *ICML*, 2021.

Croce, F., Andriushchenko, M., Sehwag, V., Debenedetti, E., Flammarion, N., Chiang, M., Mittal, P., and Hein, M. Robustbench: a standardized adversarial robustness benchmark. In *Thirty-fifth Conference on Neural Information Processing Systems Datasets and Benchmarks Track (Round 2)*, 2021. URL <https://openreview.net/forum?id=SSKZPJCT7B>.

Dosovitskiy, A., Fischer, P., Ilg, E., Häusser, P., Hazırbaş, C., Golkov, V., v.d. Smagt, P., Cremers, D., and Brox, T. Flownet: Learning optical flow with convolutional networks. In *IEEE International Conference on Computer Vision (ICCV)*, 2015. URL <http://lmb.informatik.uni-freiburg.de/Publications/2015/DFIB15>.

Everingham, M., Van Gool, L., Williams, C. K. I., Winn, J., and Zisserman, A. The PASCAL Visual Object Classes Challenge 2012 (VOC2012) Results. <http://www.pascal-network.org/challenges/VOC/voc2012/workshop/index.html>.

Fischer, P., Dosovitskiy, A., Ilg, E., Häusser, P., Hazırbaş, C., Golkov, V., van der Smagt, P., Cremers, D., and Brox, T. Flownet: Learning optical flow with convolutional networks, 2015. URL <https://arxiv.org/abs/1504.06852>.

Gajjar, S., Hati, A., Bhilare, S., and Mandal, S. Generating targeted adversarial attacks and assessing their effectiveness in fooling deep neural networks. In *2022 IEEE International Conference on Signal Processing and Communications (SPCOM)*, pp. 1–5, 2022. doi: 10.1109/SPCOM55316.2022.9840784.

Geirhos, R., Rubisch, P., Michaelis, C., Bethge, M., Wichmann, F. A., and Brendel, W. Imagenet-trained cnns are biased towards texture; increasing shape bias improves accuracy and robustness, 2018. URL <https://arxiv.org/abs/1811.12231>.

Geirhos, R., Jacobsen, J.-H., Michaelis, C., Zemel, R., Brendel, W., Bethge, M., and Wichmann, F. A. Shortcut learning in deep neural networks. *Nature Machine Intelligence*, 2(11):665–673, nov 2020. doi: 10.1038/s42256-020-00257-z. URL <https://doi.org/10.1038%2Fs42256-020-00257-z>.

Goodfellow, I. J., Shlens, J., and Szegedy, C. Explaining and harnessing adversarial examples, 2014. URL <https://arxiv.org/abs/1412.6572>.

Grabinski, J., Keuper, J., and Keuper, M. Aliasing and adversarial robust generalization of cnns. *Machine Learning*, pp. 1–27, 2022.

Gu, J., Zhao, H., Tresp, V., and Torr, P. Segpgd: An effective and efficient adversarial attack for evaluating and boosting segmentation robustness. 2022a. doi: 10.48550/ARXIV.2207.12391. URL <https://arxiv.org/abs/2207.12391>.

Gu, J., Zhao, H., Tresp, V., and Torr, P. Segpgd: An effective and efficient adversarial attack for evaluating and boosting segmentation robustness. pp. 5, 2022b. doi: 10.48550/ARXIV.2207.12391. URL <https://arxiv.org/abs/2207.12391>.

Hariharan, B., Arbelaez, P., Bourdev, L., Maji, S., and Malik, J. Semantic contours from inverse detectors. In *International Conference on Computer Vision (ICCV)*, 2011.

Hariharan, B., Arbeláez, P., Girshick, R., and Malik, J. Hypercolumns for object segmentation and fine-grained localization. In *2015 IEEE Conference on Computer Vision and Pattern Recognition (CVPR)*, pp. 447–456, 2015. doi: 10.1109/CVPR.2015.7298642.

He, K., Zhang, X., Ren, S., and Sun, J. Deep residual learning for image recognition, 2015. URL <https://arxiv.org/abs/1512.03385>.

Hendrycks, D. and Dietterich, T. Benchmarking neural network robustness to common corruptions and perturbations, 2019. URL <https://arxiv.org/abs/1903.12261>.

Hendrycks, D., Zhao, K., Basart, S., Steinhardt, J., and Song, D. Natural adversarial examples, 2019. URL <https://arxiv.org/abs/1907.07174>.

Ilg, E., Mayer, N., Saikia, T., Keuper, M., Dosovitskiy, A., and Brox, T. Flownet 2.0: Evolution of optical flow estimation with deep networks, 2016. URL <https://arxiv.org/abs/1612.01925>.

Ilyas, A., Engstrom, L., Athalye, A., and Lin, J. Black-box adversarial attacks with limited queries and information. In *Proceedings of the 35th International Conference on Machine Learning, ICML 2018*, July 2018. URL <https://arxiv.org/abs/1804.08598>.

Iyyer, M., Wieting, J., Gimpel, K., and Zettlemoyer, L. Adversarial example generation with syntactically controlled paraphrase networks. In *Proceedings of the 2018 Conference of the North American Chapter of the Association for Computational Linguistics: Human Language Technologies, Volume 1 (Long Papers)*, pp. 1875–1885, New Orleans, Louisiana, June 2018. Association for Computational Linguistics. doi: 10.18653/v1/N18-1170. URL <https://aclanthology.org/N18-1170>.

Kang, D., Sun, Y., Hendrycks, D., Brown, T., and Steinhardt, J. Testing robustness against unforeseen adversaries, 2019. URL <https://arxiv.org/abs/1908.08016>.

Krizhevsky, A., Sutskever, I., and Hinton, G. E. Imagenet classification with deep convolutional neural networks. In Pereira, F., Burges, C., Bottou, L., and Weinberger, K. (eds.), *Advances in Neural Information Processing Systems*, volume 25. Curran Associates, Inc., 2012. URL <https://proceedings.neurips.cc/paper/2012/file/c399862d3b9d6b76c8436e924a68c45b-Paper.pdf>.

Kurakin, A., Goodfellow, I., and Bengio, S. Adversarial examples in the physical world, 2016. URL <https://arxiv.org/abs/1607.02533>.

Kurakin, A., Goodfellow, I., and Bengio, S. Adversarial machine learning at scale, 2017.

Li, Z., Liu, X., Drenkow, N., Ding, A., Creighton, F. X., Taylor, R. H., and Unberath, M. Revisiting stereo depth estimation from a sequence-to-sequence perspective with transformers. 2020a. doi: 10.48550/ARXIV.2011.02910. URL <https://arxiv.org/abs/2011.02910>.

Li, Z., Pan, H., Zhu, Y., and Qin, A. K. Pgd-unet: A position-guided deformable network for simultaneous segmentation of organs and tumors, 2020b. URL <https://arxiv.org/abs/2007.01001>.

Liu, Z., Mao, H., Wu, C.-Y., Feichtenhofer, C., Darrell, T., and Xie, S. A convnet for the 2020s, 2022. URL <https://arxiv.org/abs/2201.03545>.

Madry, A., Makelov, A., Schmidt, L., Tsipras, D., and Vladu, A. Towards deep learning models resistant to adversarial attacks, 2017. URL <https://arxiv.org/abs/1706.06083>.

Mayer, N., Ilg, E., Häusser, P., Fischer, P., Cremers, D., Dosovitskiy, A., and Brox, T. A large dataset to train convolutional networks for disparity, optical flow, and scene flow estimation. In *IEEE International Conference on Computer Vision and Pattern Recognition (CVPR)*, 2016. URL <http://lmb.informatik.uni-freiburg.de/Publications/2016/MIFDB16>. arXiv:1512.02134.

Menze, M. and Geiger, A. Object scene flow for autonomous vehicles. In *Conference on Computer Vision and Pattern Recognition (CVPR)*, 2015.

Moosavi-Dezfooli, S.-M., Fawzi, A., and Frossard, P. Deepfool: a simple and accurate method to fool deep neural networks, 2015. URL <https://arxiv.org/abs/1511.04599>.

Morris, J. X., Lifland, E., Yoo, J. Y., Grigsby, J., Jin, D., and Qi, Y. Textattack: A framework for adversarial attacks, data augmentation, and adversarial training in nlp, 2020. URL <https://arxiv.org/abs/2005.05909>.

Ribeiro, M. T., Singh, S., and Guestrin, C. Semantically equivalent adversarial rules for debugging NLP models. In *Proceedings of the 56th Annual Meeting of the Association for Computational Linguistics (Volume 1: Long Papers)*, pp. 856–865, Melbourne, Australia, July 2018. Association for Computational Linguistics. doi: 10.18653/v1/P18-1079. URL <https://aclanthology.org/P18-1079>.

Ronneberger, O., Fischer, P., and Brox, T. U-net: Convolutional networks for biomedical image segmentation, 2015. URL <https://arxiv.org/abs/1505.04597>.

Rony, J., Hafemann, L. G., Oliveira, L. S., Ayed, I. B., Sabourin, R., and Granger, E. Decoupling direction and norm for efficient gradient-based l2 adversarial attacks and defenses, 2019.

Schmalfuss, J., Scholze, P., and Bruhn, A. A perturbation-constrained adversarial attack for evaluating the robustness of optical flow, 2022. URL <https://arxiv.org/abs/2203.13214>.

Schrodi, S., Saikia, T., and Brox, T. Towards understanding adversarial robustness of optical flow networks. In *Proceedings of the IEEE/CVF Conference on Computer Vision and Pattern Recognition*, pp. 8916–8924, 2022.

Sun, Y., Chen, F., Chen, Z., and Wang, M. Local aggressive adversarial attacks on 3d point cloud, 2021. URL <https://arxiv.org/abs/2105.09090>.

Teed, Z. and Deng, J. Raft: Recurrent all-pairs field transforms for optical flow, 2020. URL <https://arxiv.org/abs/2003.12039>.

Vo, J., Xie, J., and Patel, S. Multiclass asma vs targeted pgd attack in image segmentation, 2022. URL <https://arxiv.org/abs/2208.01844>.

Wong, A., Cicek, S., and Soatto, S. Targeted adversarial perturbations for monocular depth prediction. In *Advances in neural information processing systems*, 2020a.

Wong, E., Rice, L., and Kolter, J. Z. Fast is better than free: Revisiting adversarial training, 2020b. URL <https://arxiv.org/abs/2001.03994>.

Wulff, J., Butler, D. J., Stanley, G. B., and Black, M. J. Lessons and insights from creating a synthetic optical flow benchmark. In A. Fusiello et al. (Eds.) (ed.), *ECCV Workshop on Unsolved Problems in Optical Flow and Stereo Estimation*, Part II, LNCS 7584, pp. 168–177. Springer-Verlag, October 2012.

Xie, S., Girshick, R., Dollár, P., Tu, Z., and He, K. Aggregated residual transformations for deep neural networks, 2016. URL <https://arxiv.org/abs/1611.05431>.

Xu, H., Ma, Y., Liu, H., Deb, D., Liu, H., Tang, J., and Jain, A. K. Adversarial attacks and defenses in images, graphs and text: A review, 2019. URL <https://arxiv.org/abs/1909.08072>.

Zhang, J., Chen, L., Liu, B., Ouyang, B., Xie, Q., Zhu, J., Li, W., and Meng, Y. 3d adversarial attacks beyond point cloud, 2021. URL <https://arxiv.org/abs/2104.12146>.

Zhao, H. semseg. <https://github.com/hszhao/semseg>, 2019.

Zhao, H., Shi, J., Qi, X., Wang, X., and Jia, J. Pyramid scene parsing network, 2016. URL <https://arxiv.org/abs/1612.01105>.

Zhao, H., Shi, J., Qi, X., Wang, X., and Jia, J. Pyramid scene parsing network. In *CVPR*, 2017.

A. Experimental Results.

Here we report the entire quantitative results that have already been presented in the main paper. For more qualitative results on optical flow, please also refer to the video we provide in the supplementary material.

A.1. Semantic Segmentation

For the results reported in figures 2, 3, we report the results in a table here in tables 3, 4 respectively.

Table 3: Comparison of performance of CosPGD to SegPGD for semantic segmentation over PASCAL VOC2012 validation dataset. We observe that CosPGD is a stronger attack than SegPGD for both metrics, and models.

Network	Attack method	Attack iterations									
		3		5		10		20		40	
		mIoU(%)	mAcc(%)	mIoU(%)	mAcc(%)	mIoU(%)	mAcc(%)	mIoU(%)	mAcc(%)	mIoU(%)	mAcc(%)
UNet	SegPGD	36.07	57.29	21.20	50.32	12.53	41.09	8.89	34.49	6.78	28.84
	CosPGD	18.11	36.29	12.12	27.10	7.99	19.28	6.53	16.52	5.49	14.19
PSPNet	SegPGD	24.20	55.92	15.40	46.63	10.02	36.18	8.46	32.54	8.05	31.27
	CosPGD	13.13	33.19	7.10	22.19	4.89	18.23	3.96	16.33	3.83	16.31

Table 4: Comparison of performance of one-step CosPGD to FGSM for semantic segmentation over PASCAL VOC2012 validation dataset using UNet and PSPNet. As shown in Fig. 5 and explained in Sec. 4.2, images produced by FGSM attack from $\epsilon = 1.0$ onward are very noisy, thus FGSM fails as an effective adversarial point from there.

Network	Attack method	Attack epsilon													
		0.1		0.2		0.3		1.0		2.0		3.0		4.0	
		mIoU(%)	mAcc(%)	mIoU(%)	mAcc(%)	mIoU(%)	mAcc(%)	mIoU(%)	mAcc(%)	mIoU(%)	mAcc(%)	mIoU(%)	mAcc(%)	mIoU(%)	mAcc(%)
UNet	FGSM	41.24	62.73	39.89	59.65	38.22	55.55	13.61	18.02	3.81	5.02	3.56	4.75	3.55	4.76
	CosPGD	39.79	59.97	37.12	57.62	34.40	54.87	21.72	38.06	9.45	18.22	4.91	7.39	3.75	4.94
PSPNet	FGSM	42.35	66.38	40.59	63.11	36.67	56.88	3.37	7.83	3.50	5.11	3.52	4.70	3.56	4.75
	CosPGD	38.03	62.39	33.88	59.11	30.17	55.40	10.06	24.34	2.01	10.60	0.30	3.54	0.45	2.03

A.2. Optical flow estimation

Here we report the results comparing one-step CosPGD to FGSM using RAFT for KITTI15 and Sintel datasets in Table 5. We additionally submit a video comparing CosPGD to PGD over Sintel and KITTI15 datasets. We observe, that due to the high image quality of the datasets, even at high attack intensities, the input images look similar to the original (unperturbed) images despite having a lower $PSNR \approx 40db$.

Table 5: Comparison of performance of one-step CosPGD to FGSM for optical flow estimation over KITTI15 and Sintel validation datasets using RAFT.

Attack epsilon	KITTI15				Sintel			
	FGSM		one-step CosPGD		FGSM		one-step CosPGD	
	epe↑	f1-all↑	epe↑	f1-all↑	clean epe↑	final epe↑	clean epe↑	final epe↑
0.1	2.16	8.38	2.19	8.52	1.287	2.19	1.293	2.22
0.2	2.53	11.09	2.55	11.20	1.624	2.66	1.631	2.68
0.3	2.83	13.59	2.85	13.67	1.874	3.01	1.883	3.03
1.0	4.10	29.59	4.13	29.64	3.208	4.46	3.181	4.49
5.0	6.42	64.50	6.64	64.05	6.77	7.60	7.72	9.16
8.0	7.45	71.48	7.87	71.13	9.57	9.15	10.24	12.045

Following the work by Teed & Deng (2020), $f1 - all$ is calculated by averaging out over all the predicted optical flows. out is calculated using equation 5,

$$out = epe > 3.0 \cup \frac{epe}{mag} > 0.05 \quad (5)$$

Where, $mag = \sqrt{flow \ ground \ truth^2}$

B. Ablation Study

Following, we ablate over the hyperparameter α (step size) as it has a significant role in determining the strength of iterative adversarial attacks. Since, the magnitudes of cosine similarities between the vectorized prediction and target are significantly lower than comparing prediction and target masks, as in the case of SegPGD, it warrants a higher step size. This enables CosPGD to create strong adversaries at low and high attack intensities.

B.1. Step Size

Table 6: Ablation over hyperparameter step-size α for semantic segmentation using UNet over PASCAL VOC2012 validation dataset of the proposed CosPGD.

Step Size α	Attack iterations											
	3		5		10		20		40		100	
	mIoU(%)	mAcc(%)	mIoU(%)	mAcc(%)	mIoU(%)	mAcc(%)	mIoU(%)	mAcc(%)	mIoU(%)	mAcc(%)	mIoU(%)	mAcc(%)
0.15	18.11	36.29	12.12	27.10	7.99	19.28	6.53	16.52	5.49	14.19	4.76	11.87
0.10	19.75	39.51	13.48	30.24	9.17	22.15	7.26	18.48	6.11	16.10	5.15	12.57
0.07	21.14	41.88	14.81	32.85	9.98	24.01	7.54	19.09	6.40	16.83	5.34	12.79
0.01	36.84	58.54	27.60	49.68	18.24	38.71	13.08	30.45	9.88	24.56	7.38	18.13

We compare the attack strength of CosPGD over various α in table 6 and use SegPGD as the baseline. We observe, at low $\alpha(= 0.01)$, CosPGD gets stronger with more iterations, however, is not as strong as SegPGD. As we increase α to 0.07 and 0.1, we observe that CosPGD is significantly stronger than SegPGD at the low number of iterations. But, the gap closes as we increase the number of iterations, on reaching 100 iterations, SegPGD becomes a stronger attack. Thus, we increase the value of α to 0.15. This is when CosPGD significantly outperforms SegPGD at all attack iterations. We chose this value of step-size α for all iterative CosPGD attacks across tasks. Increasing the step size α always leads to a drop in model performance, across all metrics. This helps as a sanity check, that increasing α leads to a stronger attack while keeping perturbation size within the same ϵ -ball ($\epsilon = 0.03$).